# Activated carbon derived from coffee waste as supercapacitor electrode material

**Omkar Khadka*, Umesh Lawaju**, Sunil Koju*, Ram Chandra Rai***, Mim Lal Nakarmi**** and Prakash Joshi*****

*Department of Physics, Amrit Science Campus, Tribhuvan University, Kathmandu, Nepal.

**Department of Physics, Patan Multiple Campus, Tribhuvan University, Lalitpur, Nepal.

***Department of Physics, SUNY Buffalo State, Buffalo, NY 14222, USA.

****Department of Physics, Brooklyn College and the Graduate Center of the City University of New York, Brooklyn, NY 11210, USA.

*****Department of Physics, Bhaktapur Multiple Campus, Tribhuvan University, Bhaktapur, Nepal.

**Abstract:** Activated carbon prepared from waste coffee (seed powder) was investigated as a potential low-cost electrode material for supercapacitors. Energy Dispersive X-ray Spectroscopy (EDS) of the activated carbon detected the presence of a high amount of carbon (~93.9%) and oxygen (~5.2%). X-ray diffraction (XRD) analysis indicated the presence of graphitic carbon whereas Raman spectra showed a slightly greater content of amorphous carbon than graphitic carbon. Nitrogen adsorption-desorption isotherm of the activated carbon revealed that most of the pores in the activated carbon were micropores. The dominant pore width calculated from the Density Functional Theory (DFT) and Brunauer-Emmett-Teller (BET) surface area of the activated carbon were measured to be 1.61 nm and 825.5 $m^2g^{-1}$, respectively. The electrochemical characterization was performed by cyclic voltammetry and galvanostatic charge-discharge test in 3 M KOH electrolyte. The activated carbon electrode obtained a specific capacitance of 113.81 F $g^{-1}$ at 1 A $g^{-1}$. Thus, activated carbon from waste coffee could be a promising low-cost electrode material for supercapacitors.

**Keywords:** Activated carbon; Supercapacitor; Waste coffee.

## Introduction

Supercapacitors or ultracapacitors are energy storage devices that tend to fill a gap between capacitors and batteries with its power density higher than batteries and its energy density higher than capacitors[1]. However, its energy density needs to be much higher to match the energy density of batteries. Nonetheless, supercapacitors find their application in automobiles, portable electronic gadgets, etc. due to their excellent cyclability, fast charge-discharge capability, and long-term stability[2–8]. Supercapacitors, based on their energy-storing mechanisms, are classified into electric double-layer capacitors (EDLCs) and pseudocapacitors. The former stores energy by separating charge in Helmholtz double-layer across the interface of electrodes and electrolytes[8] whereas the latter uses electrosorption, reduction-oxidation reactions, and intercalation processes to store energy[9].

EDLCs use various carbonaceous materials such as carbon black[10], lampblack[11], graphene[12], carbon nanotubes[13], mesoporous carbon microspheres[14], and activated carbon[2,3,5,7,8,15,16] as electrode materials. Among them activated carbon has been widely used because of its easy synthesis, low cost, large surface area, and porous structure.

Activated carbons derived from biomass such as corncob[2,4], cotton stalk[17], wood of *Shorea robusta*[16], agar[5], pollen-cone[7], lapsi seed[18] etc., have been proposed as potential electrode material for supercapacitors. Each biomass derived activated carbon has different ratios of micropores and mesopores due to the lignocellulosic contents of the

***Author for Correspondence***: Prakash Joshi, Department of Physics, Bhaktapur Multiple Campus, Tribhuvan University, Bhaktapur, Nepal.
Email: prakash.joshi@bkmc.tu.edu.np; https://orcid.org/0000-0003-1483-2695
Received: 21 Feb, 2024; Received in revised form: 02 May, 2024; Accepted: 05 May 2024.
Doi: https://Doi.org/10.3126/sw.v17i17.66416

precursor, activating agent, and activation temperature[7,16,18]. Pores of different sizes interact with the ions of the electrolyte differently. So, in the cyclic voltammetry test, microporous activated carbons have high capacitance values at low scan rates whereas mesoporous activated carbon shows high capacitance at high scan rates[19]. The precursor chosen can have an important effect on the surface texture of the activated carbon and hence on the capacitive performance of the supercapacitor. So, optimization of pore sizes, ratio of micropores and mesopores, and tuning the surface area of the activated carbon are important aspects to increase the charge storing capacity.

In this research, we use waste coffee powder as a precursor to obtain low-cost bio waste derived activated carbon. The waste coffee powder was activated using $ZnCl_2$ at an activation temperature of 700 °C. A supercapacitor electrode fabricated using the activated carbon resulted a specific capacitance of 113.81 F $g^{-1}$ at 1 A $g^{-1}$. So, the energy density of 4.78 Whkg$^{-1}$ was obtained at the power density of 137.5 Wkg$^{-1}$.

## Experimental methods

### Preparation of activated carbon

Waste coffee powder (residue obtained after making coffee beverage) from Nepal Organic Coffee Products Pvt. Ltd. was used as a precursor for the preparation of activated carbon. The coffee remnants (precursor) were washed with distilled water and dried in an oven at 70 °C for 24 hours. The precursor was chemically activated with an aqueous $ZnCl_2$ solution with a precursor to $ZnCl_2$ mass ratio of 1:1. The activated precursor was left for 24 hours and then dried prior to the carbonization process. The activated precursor was then carbonized in an inert nitrogen atmosphere at 700 °C in a tube furnace for 4 hours. After carbonization, the sample was washed with 0.1 M HCl and then with deionized water till the pH of the water became neutral (6.5–7.5). The activated carbon was dried, ground, and filtered for further characterization and preparation of the supercapacitor electrode.

### Material Characterization

The study of the surface morphology of the waste coffee based activated carbon was carried out using scanning electron microscopy (SEM) and its elemental composition was determined from the EDS system in the SEM using the FEI Helios Nanolab 660 scanning electron microscope, Thermo Fisher Scientific, USA. The structural properties were studied by XRD analysis using the Rigaku MiniFlex 600 diffractometer with the Cu Kα source (λ = 1.54 Å). Raman spectroscopy was used to determine the relative disorder of carbons in the sample. The surface area and pore size distributions of the sample were measured using Autosorb-1C, Quantachrome, USA.

### Fabrication of activated carbon-based working electrode and electrochemical measurement

Supercapacitor electrodes were prepared using the activated carbon derived from the coffee waste powder. For this purpose, activated carbon powder weighing 4 mg, polyvinylidene fluoride (PVDF) (bought from Apollo Scientific and used as binder) and carbon black weighing 0.5 mg each were mixed in a mortar. After adding 250 µL of 1-Methyl-2-pyrrolidinone (NMP) solution (Purchased from Glentham Life Sciences), the mixture was ground thoroughly to obtain a slurry. The mixed slurry was then applied to a nickel foam and dried overnight at 70 ºC in an oven. The NMP solution was used to disperse the PVDF powder. The carbon black served as a conductor material. The prepared electrodes were then pressed and immersed in 3 M aqueous potassium hydroxide (KOH) for about 12 hours.

The immersed electrodes were taken out and used as a working electrode in a three-electrode system in which Ag/AgCl was used as the reference electrode, platinum wire as the counter electrode, and 3 M aqueous KOH solution as the electrolyte. Cyclic Voltammetry (CV) and galvanostatic charge-discharge (GCD) tests were performed using Interface 1010E (Gamry Instrument, USA). The CV measurement was carried out in the potential range of -0.2 V to -1 V at various scan rates. The GCD tests were

performed at a current density from 1 $Ag^{-1}$ to 5 $Ag^{-1}$ in the voltage range of -1.1 V to 0 V.

For CV analysis, the specific capacitance of the electrodes was calculated as[16],

$$C_{sp} = \frac{A}{2km\Delta V} \qquad (1)$$

where $C_{sp}$ is the specific capacitance (F $g^{-1}$), A is the area under curve (A.V), k is scan rate ($Vs^{-1}$), m is the mass in the electrode (g), and ΔVis the potential window (V).

For GCD tests, the specific capacitances were calculated as[16],

$$C_{sp} = \frac{I\Delta t}{m\Delta V} \qquad (2)$$

where $C_{sp}$ is the specific capacitance (F $g^{-1}$), I is the current (A), Δt is the discharge time (s), m is the mass in the electrode (g), and ΔV is the potential window (V).

The energy density (E) and power density (P) of the electrodes were calculated as[16],

$$E = \frac{1}{8} C_{sp} \Delta V^2 \qquad (3)$$

$$P = \frac{E}{\Delta t} \qquad (4)$$

where $C_{sp}$ is specific capacitance, ΔV is the potential window (V), and Δt is the discharge time (s).

## Results and discussion

### Characterization of the material

Figure 1 shows the SEM images of the activated carbon of waste coffee carbonized at 700 °C in different magnifications. Micron size distinct pores can be clearly seen in the carbon particle as depicted in the SEM image in Figure 1(a). The SEM image with higher magnification (~2000 times) in Figure 1(b), shows the rough surface morphology of the activated carbon.

In order to explore the elemental compositions of the activated carbon, SEM-EDS of the activated carbon was carried out at several sites on the sample and average values were calculated. Figure 2 is a typical energy dispersive x-ray spectrum of the activated carbon prepared from the coffee powder. The spectrum shows that the carbon sample contains an average ~93.9 % carbon, ~5.2 % oxygen by atomic weight and some traces of chlorine, sulfur, and silicon. The dominant chemical component present in activated carbon is carbon. The presence of oxygen may be

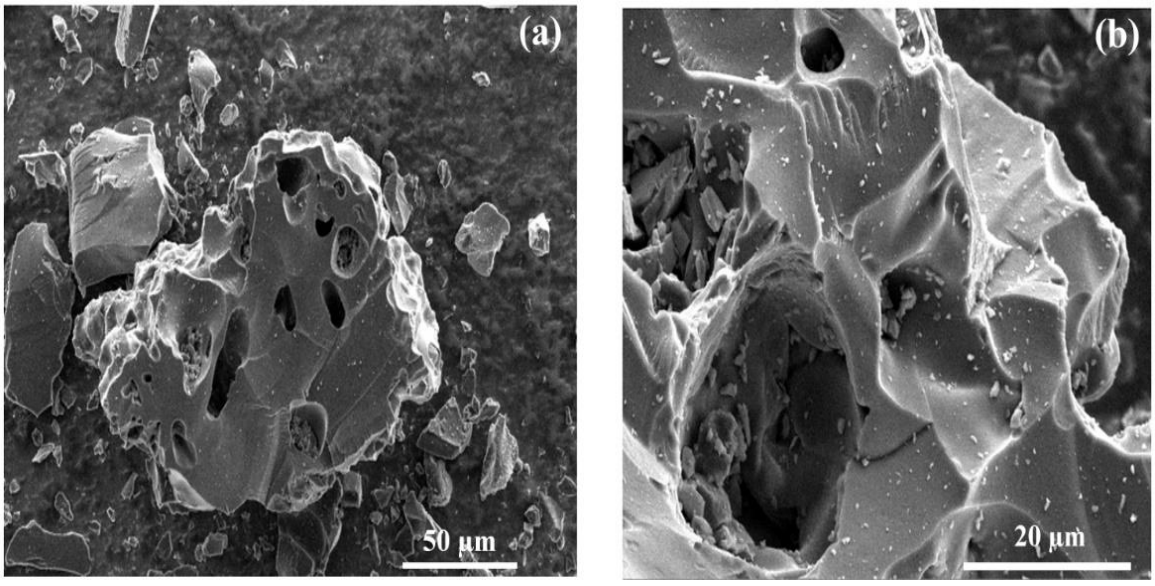


**Figure 1: SEM images of the activated carbon of waste coffee powder carbonized at 700 °C with a) 500 times magnification b) 2000 times magnification.**

due to the absorbed water vapor from the air and oxygen containing functional groups in the sample. Other traces of elements may be due to the organic nature of the precursor which is also reported by other authors[20].

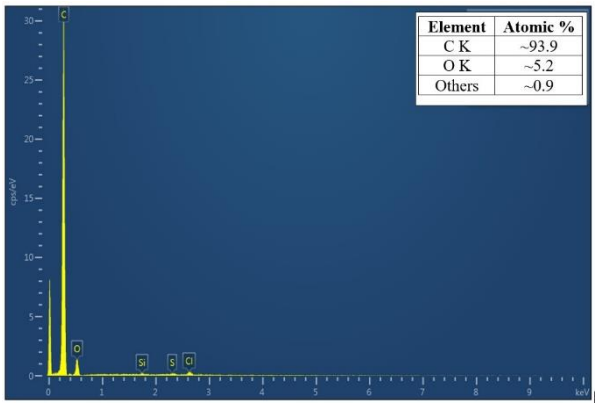


**Figure 2: Typical energy dispersive x-rays spectroscopy spectrum (EDS) of activated carbon.**

The structural composition of the activated carbon was carried out by using X-ray diffraction (XRD). The XRD pattern of activated carbon is displayed in Figure 3. The XRD pattern shows two distinct peaks at $2\theta$ ~ 25° and 43° which correspond to the (002) and (100) planes, respectively[21]. This indicates that the activated carbon of the coffee waste contains graphitic carbon[18,21]. The sharp peak at $2\theta$ ~ 48° and a smaller peak at around 36 ° are due to the ZnO nanoparticles formed during the activation of coffee carbon by $ZnCl_2$[22].

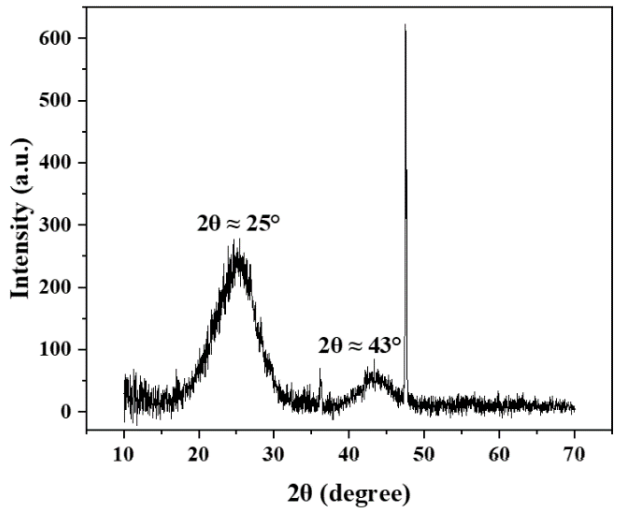


**Figure 3: XRD spectrum (baseline corrected) of activated carbon prepared with waste coffee.**

Figure 4 shows the Raman spectrum of the activated carbon. The peak fitting of Raman spectrum shows two distinct peaks centered around wavenumber of ~1338 and ~1591 $cm^{-1}$, corresponding to the D-band and G-band, respectively[7,16]. The D-band corresponds to disordered carbon and the G-band corresponds to ordered graphitic layers[7,23]. The disordered carbon act as active sites for ion adsorption and electrochemical reactions whereas ordered graphitic layers provides good electrical conductivity but reduces active sites[24–26].

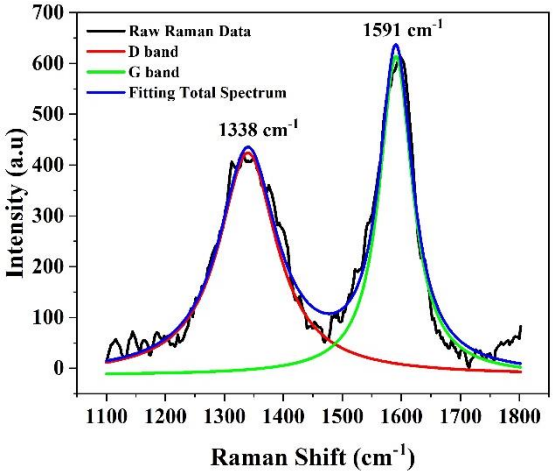


**Figure 4: Raman spectrum and peak fitting of activated carbon prepared with waste coffee.**

The higher Raman shifts values of D-band and G-band indicate a shorter bond length between atoms which helps in fast charge transfer ability[26]. The Raman spectrum is fitted using Lorentzian line shapes with background subtraction[27]. The activated carbon contains about 54.92 % disordered carbon and 45.08 % ordered crystalline carbon which indicates that the content of amorphous carbon is slightly greater than, or at least equal to that of the graphitic layers.

The $N_2$ adsorption-desorption isotherm of the activated carbon, shown in Figure 5 is similar to the type I characteristics of microporous material. The weak hysteresis loop at 0.6 - 0.8 $P/P_o$ indicates the presence of mesoporous structures as well[5]. So, the majority of the pores in the activated carbon are micropores with a small number of mesopores. Brunauer-Emmett-Teller (BET) surface area,

micropore volume, pore width, and pore volume are listed in table 1. The specific surface area of the activated carbon is found to be 825.5 $m^2g^{-1}$. The total pore volume obtained from the Density Functional Theory (DFT) method[28] is 0.4946 cc $g^{-1}$ and micropore volume obtained from t-method is 0.3564 cc $g^{-1}$. The maximum number of pores has a microporous width of 1.6137 nm validating the $N_2$ isotherm. The ratio of micropore area to the specific surface area is 82.69 %, which indicates high concentration of micropores in the sample.

**Table 1: Specific surface area and pore characteristics of activated carbon.**

| $S_{BET}$ ($m^2g^{-1}$) | $S_{micro}$ ($m^2g^{-1}$) | $S_{micro}/S_{BET}$ | $V_{micro}$ (cc $g^{-1}$) | $W_{DFT}$ (nm) | $V_{DFT}$ (cc $g^{-1}$) |
|---|---|---|---|---|---|
| 825.5 | 682.6 | 82.69% | 0.3564 | 1.6137 | 0.4946 |

$S_{BET}$ = specific surface area, $S_{micro}$ = micropore area, $V_{micro}$ = micropore volume using t-method, $W_{DFT}$ = pore width (mode) using DFT method, $V_{DFT}$ = pore volume using DFT analysis

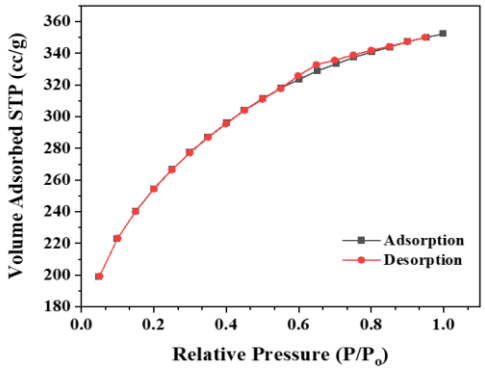


**Figure 5: Nitrogen adsorption-desorption isotherm.**

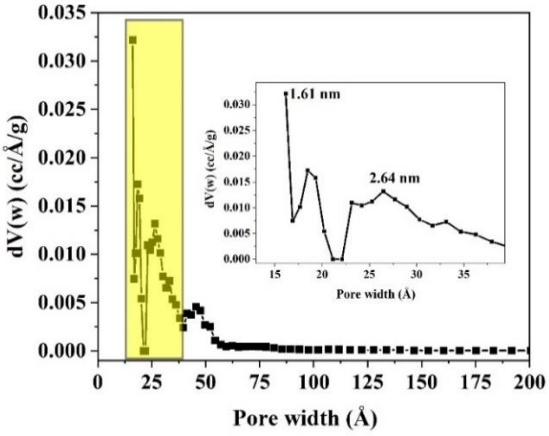


**Figure 6: Pore size distribution obtained by DFT method.**

Figure 6 show the pore size distribution obtained from the DFT method which indicates the presence of higher number of microporous structures with a pore size of ~1.61 nm. From the Figure, it can be seen that the activated carbon also contains mesopores structures. So, there exists both microporous and mesoporous structure in the activated carbon of coffee waste.

## Electrochemical properties

Figure 7 shows the cyclic voltammogram of waste coffee based activated carbon. The CV curves of the activated carbon exhibited a quasi-rectangular shape with no redox peak. That is the characteristics of the electric double layer capacitor (EDLC) [6]. Also, even at high scan rate of 100 $mVs^{-1}$, the CV curve maintains the characteristic rectangular shape indicating good charge transfer ability[5].

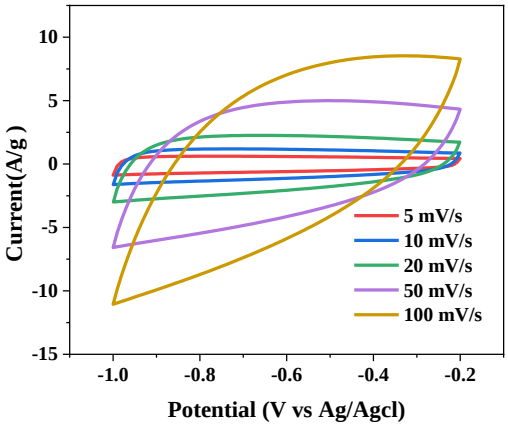


**Figure 7: CV of coffee activated carbon electrode at different scan rates.**

The specific capacitance at scan rates of 5, 10, 20, 50 and 100 $mVs^{-1}$ is 109.11, 101.90, 91.62, 70.19 and 47.55 F $g^{-1}$, respectively. This result shows the decrease of specific capacitance as the scan rate is increased. It is because the ions have sufficient time to diffuse through the surface of

the micropores at slow scan rates. But at high scan rate, the ions require pores with larger size to enter into the electrode's surface and less electrochemically active surface area of the pores are utilized[6]. Thus, the micropores store the charges and mesopores help with the fast accessibility of ions.

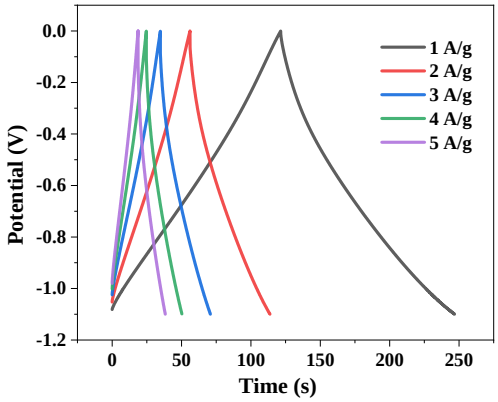


**Figure 8: GCD curves of waste coffee based activated carbon at different current densities.**

Figure 8 shows the GCD curves of the coffee based activated carbon at various current densities. The specific capacitance of the waste coffee based activated carbon electrode at 1, 2, 3, 4, and 5 A $g^{-1}$ are 113.81, 104.73, 98.21, 93.2 and 89 F $g^{-1}$, respectively. There was only 21.8 % decrease in the specific capacitance as the current density is increased from 1 to 5 A $g^{-1}$ indicating excellent capacitive performance during the rapid charge and discharge operations. This is due to the presence of both micropores and mesopores in the activated carbon as indicated by the DFT analysis. All of the curves in the charge and discharge regions preserve their ideal linear shapes indicating ideal capacitive behavior and hence, confirms the double layer formation on the electrode electrolyte interface. The IR drop is also very small indicating small internal resistance and hence low energy dissipation of the capacitor[29].

Figure 9 shows the Ragone plot of activated carbon electrode at current densities ranging from 1 to 5 A $g^{-1}$. At the current density of 1 A $g^{-1}$, the energy density and power density are found to be 4.78 Whkg$^{-1}$ and 137.5 Wkg$^{-1}$, respectively, which is similar to the result obtained by Shrestha *et al.*[16]

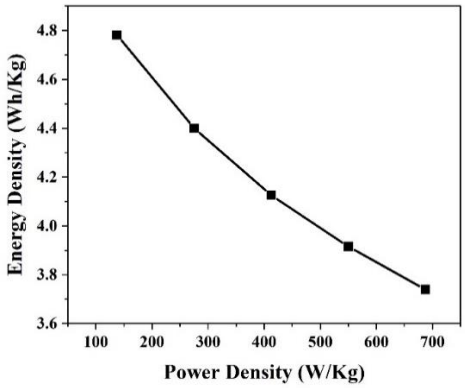


**Figure 9: Ragone plot at different current densities.**

The specific capacitance depends on the specific surface area and the porosity of the electrode material[8]. High specific surface area provides large active sites whereas suitable pore structures enhance electrolyte diffusion and material utilization. Since the activated carbon of the coffee waste contain mesoporous structures for fast transfer of ions and microporous structures for large electrochemically active surface area, the activated carbon electrode possesses high-rate capability as shown by the GCD curves. The obtained specific capacitance of 113.81 F $g^{-1}$ at 1 A $g^{-1}$ is comparable, if not higher than the literature. For example, Chiu *et al.* compared different activating agents such as $ZnCl_2$ for activation of coffee waste grounds and reported a specific capacitance of 72.9 F $g^{-1}$ at 0.5 A $g^{-1}$ [26]. Similarly, Adan-Mas *et al.* used KOH as an activating agent for the activation of waste coffee ground and reported a specific capacitance of 84 F $g^{-1}$ at 1 A $g^{-1}$ [21]. So, due to its high carbon concentration, incorporation of both microporous and mesoporous structures, and shorter bond length between carbon atoms, activated carbon obtained from waste coffee is a good candidate for supercapacitor electrodes.

## Conclusion

In this research, low cost activated carbon derived from waste coffee (residue) was successfully prepared using the chemical activation method and used to prepare supercapacitor electrodes. The XRD revealed the presence of graphitic carbon and the Raman spectroscopy indicated the availability of nearly equal amount of conducting

carbon and active sites for ion adsorption. Also, the shorter bond length between carbon atoms facilitates fast charge transfer. The activated carbon contained both microporous and mesoporous structure with the former having a higher concentration which helped in the rapid charge discharge capability. So, the prepared electrodes showed excellent electric double layer capacitor behavior with a specific capacitance of 113.81 F $g^{-1}$ at 1 A $g^{-1}$. Thus, the activated carbon can be used to make low-cost supercapacitor electrode for high power applications.

**Acknowledgments**

The authors are thankful to Associate Professor Sudarshana Shakya, Bhaktapur Multiple Campus (BMC), Prof. Nishith Verma and Rahul Gupta (Research Scholar), Environmental Remediation Lab, Indian Institute of Technology (IIT), Kanpur, India. Prof. Sarang Ingole, and Dr. Shiva Kant, department of MSE, IIT, Kanpur, India. One of the authors would like to acknowledge for the support from PSC-CUNY grant.

**References**

1. Kötz, R. and Carlen, M. 2000. Principles and applications of electrochemical capacitors. *Electrochimica Acta* **45**(15): 2483–2498.
   Doi: https://doi.org/10.1016/S0013-4686(00)00354-6.
2. Yang, S. and Zhang, K. 2018. Converting corncob to activated porous carbon for supercapacitor application. *Nanomaterials* **8**(4): 181.
   Doi: https://doi.org/10.3390/nano8040181.
3. He, X. et al. 2009. Preparation of microporous activated carbon and its electrochemical performance for electric double layer capacitor. *Journal of Physics and Chemistry of Solids*. **70**(3): 738–744.
   Doi: https://doi.org/10.1016/j.jpcs.2009.03.001.
4. Karnan, M. et al. 2017. Electrochemical studies on corncob derived activated porous carbon for supercapacitors application in aqueous and non-aqueous Electrolytes. *Electrochimica Acta.* **228**: 586–596.
   Doi: https://doi.org/10.1016/j.electacta.2017.01.095.
5. Guo, Y. et al. 2021. Agar-Based porous electrode and electrolyte for flexible symmetric supercapacitors with ultrahigh energy density. *Journal of Power Sources.* **507**: 230252.
   Doi: https://doi.org/10.1016/j.jpowsour.2021.230252.
6. Xing, W. et al. 2006. Superior electric double layer capacitors using ordered mesoporous carbons. *Carbon.* **44**(2): 216–224.
   Doi: https://doi.org/10.1016/j.carbon.2005.07.029.
7. hor, a. a., and hashmi, s. a. 2020. optimization of hierarchical porous carbon derived from a biomass pollen-cone as high-performance electrodes for supercapacitors. *Electrochimica Acta*. **356**: 136826.
   Doi: https://doi.org/10.1016/j.electacta.2020.136826.
8. Qu, D. and Shi, H. 1998. Studies of activated carbons used in double-layer capacitors. *Journal of Power Sources.* **74**(1): 99–107.
   Doi: https://doi.org/10.1016/S0378-7753(98)00038-X.
9. Conway, B. E., Birss, V., and Wojtowicz, J. 1997. The role and utilization of pseudocapacitance for energy storage by supercapacitors. *Journal of Power Sources.* **66**(1): 1–14.
   Doi: https://doi.org/10.1016/S0378-7753(96)02474-3.
10. Krause, A. et al. 2011. Electrochemical double layer capacitor and lithium-ion capacitor based on carbon black. *Journal of Power Sources.* **196**(20): 8836–8842.
    Doi: https://doi.org/10.1016/j.jpowsour.2011.06.019.
11. Lawaju, U., Kc, A. and Joshi, P. 2023. Lampblack of soybean oil as a low-cost electrode material in supercapacitor application. *Scientific World*. **16**(16): 94–99.
    Doi: https://doi.org/10.3126/sw.v16i16.56828.
12. Schütter, C. et al. 2014. Activated carbon, carbon blacks and graphene based nanoplatelets as active materials for electrochemical double layer capacitors: A comparative study. *J. Electrochem. Soc.* **162**(1): A44.
    Doi: https://doi.org/10.1149/2.0381501jes.
13. Wang, G. et al. 2014. Improving the specific capacitance of carbon nanotubes-based supercapacitors by combining introducing functional groups on carbon nanotubes with using redox-active electrolyte. *Electrochimica Acta.* **115**: 183–188.
    Doi: https://doi.org/10.1016/j.electacta.2013.10.165.
14. Xiong, W. et al. 2011. A novel synthesis of mesoporous carbon microspheres for supercapacitor electrodes. *Journal of Power Sources.* **196**(23): 10461–10464.
    Doi: https://doi.org/10.1016/j.jpowsour.2011.07.083.
15. Barbieri, O. et al. 2005. Capacitance limits of high surface area activated carbons for double layer capacitors. *Carbon.* **43**(6): 1303–1310.
    Doi: https://doi.org/10.1016/j.carbon.2005.01.001.
16. Shrestha, D. et al. 2019. Shorea robusta derived activated carbon decorated with manganese dioxide hybrid composite for improved capacitive behaviors. *Journal of Environmental Chemical Engineering*. **7**(5): 103227.
    Doi: https://doi.org/10.1016/j.jece.2019.103227.
17. Chen, M. et al. 2013. Preparation of activated carbon from cotton stalk and its application in supercapacitor. *J Solid State Electrochem.* **17**(4): 1005–1012.
    Doi: https://doi.org/10.1007/s10008-012-1946-6.

18. Shrestha, L. K. et al. 2020. High surface area nanoporous graphitic carbon materials derived from lapsi seed with enhanced supercapacitance. *Nanomaterials* **10**(4): 728. Doi: https://doi.org/10.3390/nano10040728.
19. Zheng, C. et al. 2010. Cooperation of micro- and meso-porous carbon electrode materials in electric double-layer capacitors. *Journal of Power Sources*. **195**(13): 4406–4409. Doi: https://doi.org/10.1016/j.jpowsour.2010.01.041.
20. Awe, A. A. et al. 2020. Preparation and characterisation of activated carbon from vitisvinifera leaf litter and its adsorption performance for aqueous phenanthrene. *Applied Biological Chemistry*. **63**(1): 12. Doi: https://doi.org/10.1186/s13765-020-00494-1.
21. Adan-Mas, A. et al. 2021. Coffee-derived activated carbon from second biowaste for supercapacitor applications. *Waste Management*. **120**: 280–289. Doi: https://doi.org/10.1016/j.wasman.2020.11.043.
22. Yogamalar, R. et al. 2009. X-Ray peak broadening analysis in zno nanoparticles. *Solid State Communications*. **149**(43): 1919–1923. Doi: https://doi.org/10.1016/j.ssc.2009.07.043.
23. Joshi, P. 2017. Novel counter electrodes of dye-sensitized solar cells based on activated carbon prepared from wood of choerospondias axillaris seed-stones and alnus nepalensis plant. *Int. J. Eng. Adv. Res. Tech.* **3**(3): 8–11.
24. Miyata, Y., Mizuno, K., and Kataura, H. 2010. Purity and defect characterization of single-wall carbon nanotubes using raman spectroscopy. *Journal of Nanomaterials*. **2011**: e786763. Doi: https://doi.org/10.1155/2011/786763.
25. Liu, Y. et al. 2018. Shape-controlled synthesis of porous carbons for flexible asymmetric supercapacitors. *Nanoscale*. **10**(48): 22848–22860. Doi: https://doi.org/10.1039/C8NR06966B.
26. Chiu, Y.-H. and Lin, L.-Y. 2019. Effect of activating agents for producing activated carbon using a facile one-step synthesis with waste coffee grounds for symmetric supercapacitors. *Journal of the Taiwan Institute of Chemical Engineers*. **101**: 177–185. Doi: https://doi.org/10.1016/j.jtice.2019.04.050.
27. K.c., A. et al. 2023. Heterogeneous integration of high-quality diamond on aluminum nitride with low and high seeding density. *Journal of Crystal Growth*. **610**: 127172. Doi: https://doi.org/10.1016/j.jcrysgro.2023.127172.
28. Lastoskie, C., Gubbins, K. E. and Quirke, N. 1993. Pore size distribution analysis of microporous carbons: a density functional theory approach. *J. Phys. Chem.* **97**(18): 4786–4796. Doi: https://doi.org/10.1021/j100120a035.
29. Wang, Y., Jiang, L. and Wang, Y. 2016. Development of candle soot based carbon nanoparticles (CNPs)/Polyaniline electrode and its comparative study with CNPs/MnO2 in supercapacitors. *Electrochimica Acta*. **210**: 190–198. Doi: https://doi.org/10.1016/j.electacta.2016.05.145.